

Radio Wave Penetration into Buildings – Polarization and Spatial Characteristics of the Rays

PIERRE LALY, DAVY GAILLOT, MARTINE LIENARD and PIERRE DEGAUQUE

Dept. of Electronics IEMN/TELICE

University of Lille

Bldg. P3, 59655 Villeneuve d'Ascq cedex

FRANCE

EMMERIC TANGHE and WOUT JOSEPH

Dept. iMinds

University of Gent

9050 Gent

BELGIUM

Martine.lienard@univ-lille1.fr <http://telice.univ-lille1.fr>

Abstract: - This contribution presents measurements and analysis of the outdoor-to-indoor propagation characteristics in the 1.35 GHz band. Indeed, in such a configuration, most of the results already published in the literature deal with an analysis of the path loss variation as a function of the position of the receiver inside the building, thus when it moves from a light indoor configuration to deep indoor. In this paper we extend these results to analyze the change in wave polarization, expressed in terms of cross-polar discrimination factor, and to study the distribution of the direction of the rays for many positions of the receiver inside the building. To achieve this goal, experiments have been carried out with a real time MIMO channel sounder, designed and developed by the authors, and based on flexible software architecture. After describing the main features of the sounder and the geometrical configuration of the experiments, results on narrow band and wide band analysis will be described.

Key-Words: - Outdoor-to-indoor, polarization, direction of arrival, delay spread, penetration into building

1 Introduction

The outdoor to indoor channel characteristics has already been widely studied but mainly to estimate the additional path loss when the mobile unit moves inside the building. Indeed, as outlined in [1], the way in which signals penetrate into buildings has become a central aspect of the deployment of femtocells for insuring indoor network coverage. Extensive measurements have thus been carried out to evaluate the received signal level and thus the signal to noise ratio, and to propose adequate path loss models. In [2], a study of the extra signal attenuation due to building is presented for different types of building. However, in an area close to a window, Hirota [3] points out that propagation loss does not follow the existing formula where loss is predicted in proportion to distance. Therefore, for path loss predictions, numerous models have been proposed. As an example, a theoretical analysis method that is a hybrid of ray tracing and physical optics is detailed in [4], and in [5] geometrics and finite difference methods are proposed.

Multiple Input Multiple Output (MIMO) systems can of course be used for evaluating path loss but they also allow getting a more in-depth view of the channel characteristics. In [6], MIMO measurements at 780 MHz are presented, path loss results being compared to two modified versions of COST 231 path loss model. The statistical properties of the channel matrix and of the capacity of the link are analyzed in [7], for a frequency of 3.5 GHz. In [8], angular spread and other statistical parameters characterizing the channel are discussed showing the limits of MIMO channel assumptions often used in stochastic models. However, this study was done assuming that both transmitting (Tx) and receiving (Rx) antennas are vertically polarized. Nevertheless, the polarimetric characteristics of the channel are of prime importance to exploit diversity or multiplexing schemes. Results of investigations on this point are described in [9] but only if both Tx and Rx are inside a building.

The work described in this paper is thus an extension of these previous studies and presents a

multidimensional characterization of the outdoor-to-indoor propagation, thus including both polarization and spatial aspects as the direction of arrival of the rays (DoA). A MIMO channel sounder working at a center frequency of 1.35 GHz was used, the Tx antenna illuminating the largest face of a building in which Rx is moved in different rooms. Usually, the inner environment is overall divided into two zones: light indoor (LI) and deep indoor (DI). LI deals with a configuration where Rx is in a room illuminated by the incident wave, contrary to the DI case corresponding to rooms in the center or at the opposite side of this building. The objective of this paper is to emphasize the change in the channel characteristics when Rx moves from LI to DI.

After briefly presented in Section 2 the main features of the MIMOSAS channel sounder used for the measurement campaigns, the geometrical configuration of the experiments is given in Section 3. Section 4 describes the main results in terms of polarization characteristics. Wideband analysis including DoA is presented in Section 5, Section 6 giving the conclusions derived from this work.

2 Main Features of the Channel Sounder

The MIMOSAS channel sounder was jointly developed by the University of Lille/IEMN (France) and the University of Gent/IMinds (Belgium). It is based on a flexible software architecture in which the sounding parameters can be selected depending on the studied environment [10]. Each array element is a dual-polarized patch antenna, the direction of polarization being +45° and -45°, referring to a vertical axis. The maximum number of array elements being 8, this leads to the measurement of a 16x16 channel matrix H including both polarizations. The center frequency is 1.35 GHz, the OFDM transmitted signal occupies a bandwidth of 100 MHz, the total number of subcarriers being 8192. Since the size of the Tx array can be chosen, the subcarriers can be allocated either to only one patch antenna (Single Input Multiple Output – SIMO configuration) or distributed among all Tx antennas (MIMO). For the full MIMO configuration, 1024 subcarriers feed each antenna, their spacing being equal to 97.66 kHz. The acquisition time of an H matrix is 300 µs.

The various paths and their characteristics as delay, amplitude and AoA are extracted from H by using the RiMAX high resolution algorithm.

3 Geometrical Configuration of the Experiments

A 4-element uniform linear array used for Tx was placed at a height of 5 m, the main radiation lobe of each elementary patch antenna being oriented towards a nearby building situated at a distance of 28 m. The 8-element circular Rx array was moved either in rooms facing Tx, as R1 to R4 in Fig.1, or in rooms as R5 and R6 (Deep indoor). In each of these rooms, 15 to 20 successive positions of Rx were considered. The direction of Tx is also indicated in Fig. 1. The presence of a few trees are near the windows of R2 to R4 must be emphasized since they can modify the characteristics of the incident wave. Therefore, in the following, measurements in R2 to R4 will be referred as “obstructed light indoor (OLI), R1 corresponding to Light indoor (LI). All rooms are fully equipped offices, the Rx array being moved around tables, chairs or storage cupboards.

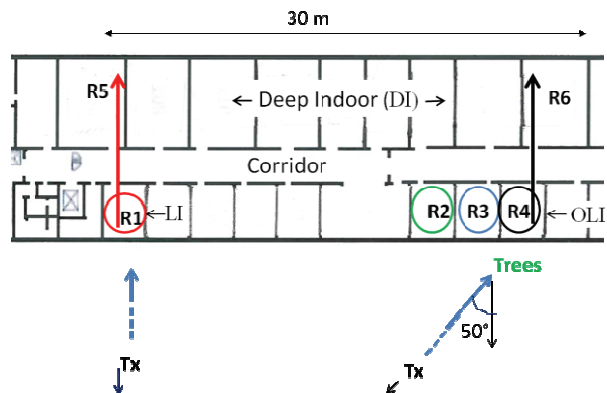


Fig. 1. Geometrical configuration of the experiments

4 Narrow Band Analysis

4.1 Path Loss and Cross Polarization Discrimination Factor

First, to provide a few figures on the additional path loss, the received power averaged over the 8 patch antennas of the Rx circular array, over all positions of this array in a room and over all frequency points of the OFDM subcarriers, has been determined. If the signal level received for LI (Room R1) is chosen as a reference, the additional attenuation for OLI (rooms R2 to R4) is 9 dB; it reaches 12 dB in the corridor and 26 dB for DI. These results were obtained for co-polarized Tx and Rx antennas.

The cross polarization discrimination factor, XPD, is defined as the ratio, often expressed in dB, between the signal received in co-polar and cross-polar configurations. Let us first consider the case where the Rx circular array is put at numerous positions in R1 (LI). For each position, XPD

averaged over the frequency band, was calculated for each elementary patch antenna of the 8-element array. Curves in Fig. 2 give the cumulative distribution function (cdf) of XPD in R1. Whatever the position of the array in the room, each antenna was identified. To enlighten the presentation in Fig. 2, only curves related to 2 specific patch antennas have been noted. “Antenna facing Tx” corresponds to the patch antenna whose main lobe is oriented towards Tx, while the “back antenna” is situated on the opposite side of the circular array. The median value of XPD is 8 dB for the antenna facing Tx, thus receiving most of the direct rays. In this case, the received signal remains linearly polarized. On the contrary, for the back antenna, waves are depolarized, the probability being even larger to receive a cross-polar component larger than for the co-polar case.

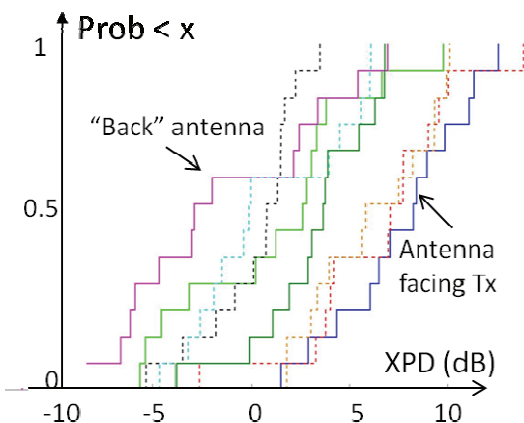


Fig. 2. Cumulative distribution function of XPD calculated for each elementary antenna of the circular array. Rx is situated in room R1, light indoor conditions.

The cdf of XPD plotted in Fig. 3 and deduced from measurements made in room R5 (DI) is quite different since the cdf is nearly the same whatever the Rx elementary patch antenna. The median value of the XPD is about 0 dB, meaning that the waves are fully depolarized.

4.2 Delay Spread

Table 1 gives the average delay spread τ for a threshold of the channel impulse response of -20 dB, referred to the highest value.

Table 1. Delay spread for various scenarios.

	Light	Deep	Light obstructed		
	R1	R5	R2	R3	R4
copol	9 ns	16 ns	13 ns	17 ns	20 ns
Xpol	19 ns	19 ns	16 ns	25 ns	28 ns

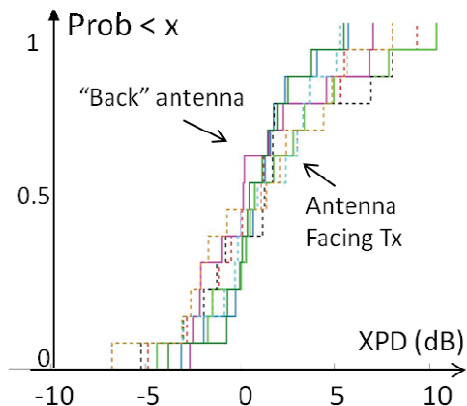


Fig. 3. Same as in Fig. 2 but for Rx in room R5, deep indoor conditions.

For co-polarized antennas, τ increases from 9 to 16 ns when Rx moves from LI to DI (R1 to R5). It must be emphasized that, even if R5 is in deep indoor, most of the powerful rays in this room are due to rays impinging the façade of the building with a nearly normal angle of incidence (Fig. 1). This has been checked by calculating the angles of departure/arrival of the rays, examples being given in Section 5.

This Table also shows that the presence of trees obstructing the LOS gives rise to an important increase of τ , reaching 20 ns in R4. An additional factor leading to such high values of τ in R3 – R4 is the increase of the angle of incidence of the direct path. Indeed, taking the distance between Tx and the illuminated wall into account, this angle of incidence reaches 50° (Fig. 1), leading to multiple reflections inside the rooms.

For cross-polarized antennas, the strongest increase of τ occurs in R1, the difference between R1 (LI) and R5 (DI) becoming negligible. This can be easily explained by the multiple reflections needed for getting a non negligible contribution of cross-polarized waves in LI configuration

5 Wideband Analysis

The main characteristics of the rays, as delay, power and direction of arrival (DoA) were deduced from measurements by applying the RiMax high resolution algorithm.

To illustrate this approach, let us consider the case of Rx moving from R1 to R5 and then from R4 to R6, as shown in Fig. 4a. The DoA of the most powerful ray received at successive positions of Rx along these 2 paths are given in Fig. 4b, the surface of the circles being proportional to the received power. The axis of reference chosen for defining the

angle of arrival is the line perpendicular to the main façade of the building (Fig. 1).

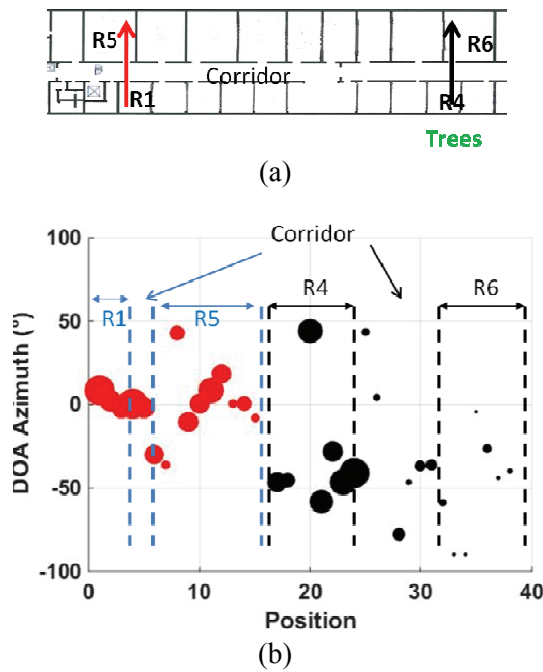


Fig. 4. (a) Geometrical configuration showing the displacement of Rx along 2 paths: R1 to R5 and R4 to R6; (b) Direction of arrival of the most powerful ray at successive receiving points along these paths.

In R1, the DoA of the most powerful ray coincides with the line Tx-Rx. In R5, the values of this DoA are still spread around 0° but sometimes reach $\pm 50^\circ$. For the second path the direction Tx-Rx is on the order of 50° (Fig.1). This mainly corresponds to the mean of the DoA but with a large dispersion around this value. This DoA is thus sometimes quite different than the direction Tx-Rx. Lastly the rms angular spread has been deduced from the DoAs of the rays and varies from about 10° in LI to 80° in DI.

4 Conclusion

The multi-dimensional channel characteristics of the outdoor-to-indoor propagation channel were measured and analyzed. For rooms situated in the line of sight of Tx (Light Indoor), wave polarization at the receiver strongly depends on the orientation of the main lobe of the Rx elementary patch antenna, referred to the direction Tx-Rx. On the contrary, for deep indoor, the waves are depolarized whatever the orientation of the antenna, the median value of the cross polarization discrimination factor being 0 dB. Delay spread for co-polarization and cross-polarization has been studied. We have also shown

that the direction of the most powerful ray is around the direction Tx-Rx but the angular spread increases from 10° for light indoor to 80° in deep indoor.

References:

- [1] D. M. Rose and T. Kurner, Outdoor to indoor propagation – Accurate measuring and modeling of indoor environment at 900 and 1800 MHz, *Proc. European Conf. Antennas and Propag. (EUCAP)*, 2012, pp. 1440-1444.
- [2] L. Ferreira, M. Kuipers, C. Rodrigues, and L. M. Correia, Characterization of signal penetration into buildings for GSM and UMTS, *Int. Symp. on Wireless communication Systems*, 2006, pp. 63-67
- [3] Y. Hirota, H. Izumikawa, and C. Ono, Outdoor-to-indoor radio propagation characteristics with 800 MHz band in an urban environment, *IEEE Ant. and Prop./URSI Symp.*, 2014, pp. 697-698
- [4] T. Imai and Y. Okumara, Study on a hybrid method of ray tracing and physical optics for outdoor-to-indoor propagation channel prediction, *IEEE Int. workshop on Electromagn.*, 2014, pp. 249-250.
- [5] G. de la Roche, P. Flipo, L. Zhuihua, G. Villemaud, Z. Jie and J. M. Gorce, Combination of geometric and finite difference models for radio wave propagation in outdoor to indoor scenarios, *European Conf. on Antennas and Propag.*, 2010, pp. 1-5
- [6] E. Suikkanen, A. Tolli and M. Latva-aho, Characterization of propagation in an outdoor-to-indoor scenario at 780 MHz, *IEEE PIMRC Symp.*, 2010, pp. 70-74.
- [7] Y. Lostanlen, T. Tenoux, H. Farhat and G. El Zein, Analysis of measured outdoor-to-indoor MIMO channel matrix at 3.5 GHz, *IEEE Ant. and Propag./URSI Symp.*, 2010, pp. 1-4.
- [8] S. Wyne, A. F. Molisch, P. Almers, G. Eriksson, J. Kardeval and F. Tufvesson, Outdoor to indoor MIMO measurements and analysis at 5.2 GHz, *IEEE Trans. Vehicular Techno.*, May 2008, pp. 1374-1386
- [9] E. M. Vitucci, F. Mani, C. Oestges and V. Degli-Esposti, Analysis and modeling of the polarization characteristics of diffuse scattering in indoor and outdoor radio propagation, *Conf. on applied EM and Commun.*, 2013, pp. 1-5.
- [10] P. Laly, D. P. Gaillot, M. Lienard, P. Degauque, E. Tanghe, W. Joseph, and L. Martens, Flexible real-time channel sounder for multidimensional polarimetric parameter estimation, *IEEE Conf. on Antenna Measur. and Applications*, Nov.30 –Dec. 2, 2015